Environmental Technology & Innovation 24 (2021) 101811

Contents lists available at ScienceDirect

Environmental Technology & Innovation

journal homepage: www.elsevier.com/locate/eti

Activated carbon with ultrahigh surface area derived from sawdust biowaste for the removal of rhodamine B in water

Van Hoang Nguyen [a], Dung T. Nguyen [b], T. Tung Nguyen [c], H. Phuong T. Nguyen [b,*], H. Binh Khuat [d], T. Hung Nguyen [d], V. Khanh Tran [d], S. Woong Chang [f], Phuong Nguyen-Tri [g], D. Duc Nguyen [e,f,*], Duc Duong La [d,*]

[a] Institute of New Technology, Nghia Do, Cau Giay, Hanoi, Vietnam
[b] School of Chemical Engineering, Hanoi University of Science and Technology, 1 Dai Co Viet, Hanoi, Vietnam
[c] Institute of Materials Science, Vietnam Academy of Science and Technology, 18-Hoang Quoc Viet, Hanoi, Vietnam
[d] Institute of Chemistry and Materials, Nghia Do, Cau Giay, Hanoi, Vietnam
[e] Faculty of Environmental and Food Engineering, Nguyen Tat Thanh University, 300A Nguyen Tat Thanh, District 4, Ho Chi Minh City, 755414, Vietnam
[f] Department of Environmental Energy Engineering, Kyonggi University, Republic of Korea
[g] Department of Chemistry, Biochemistry and Physics, Laboratory of Advanced Materials for Energy and Environment, Université du Québec à Trois-Rivieres, Québec, Canada

ARTICLE INFO

Article history:
Received 20 May 2021
Received in revised form 21 July 2021
Accepted 21 July 2021
Available online 24 July 2021

Keywords:
Sawdust
Activated carbon
Adsorption
Rhodamine B removal

ABSTRACT

Biomass has been extensively considered a sustainable resource for preparing activated carbon for energy and environmental applications. However, the fabrication of activated carbon from biomass with a high surface area that can be effectively utilized for environmental treatment remains the main drawback. In this study, activated carbon with an ultra-high surface area was fabricated from sawdust by simple, one-step chemical activation. The effects of the activating temperature and time on the surface area of the activated carbon were investigated. The sawdust activated carbon (sAC) that was obtained was characterized using scanning electron microscopy (SEM), transmission electron microscopy (TEM), X-ray diffraction (XRD), FTIR spectroscopy, and Brunauer, Emmett and Teller (BET) surface area measurements. The prepared sAC had a porous structure, which comprised aggregated nanoparticles with diameters ranging from 10 to 20 nm. The sAC exhibited a high and rapid removal efficiency toward Rhodamine B (RhB), with a removal percentage of nearly 100% after 10 min at an RhB concentration of 10 ppm. The effect of the pH solution on RhB removal performance by sawdust-activated carbon toward RhB was also investigated and discussed and showed that the sAC absorbed more than 90% of the RhB in all the pH at room temperature solutions.

1. Introduction

With the development of the global economy, synthetic colorant compounds now play a significant role in many industrial sectors, such as the food, paper, textile, leather, and pharmaceutical industries. However, these organic dyes are highly toxic because of their non-biodegradability and carcinogenic properties and can critically threaten human health

* Corresponding authors.
E-mail addresses: phuong.nguyenthihong@hust.edu.vn (H.P.T. Nguyen), nguyensyduc@gmail.com (D.D. Nguyen), duc.duong.la@gmail.com (D.D. La).

https://doi.org/10.1016/j.eti.2021.101811
2352-1864/

and ecosystems (Robinson et al., 2001; Jain et al., 2020). More than ten thousand types and nearly one million tons of organic dyes are produced annually and are increasing every year (Kamranifar et al., 2018). The most commonly used organic dyes are azo, phenothiazine and triphenylmethane derivatives used widely in industrial wastewater (Manzoor and Sharma, 2020). These dyes are stable in their chemical nature because of their stable precursors and aromatic rings. Therefore, they pose more threats to the environment and human health (Jayamani and Shanthi, 2020; Sarkar et al., 2020). Rhodamine B (RhB) is a common organic dye widely used as a fluorescent label within the water to monitor the rate and direction of transport and flow because of its easy detection and the low cost of fluorometers. Although RhB has many benefits in many industrial processes, it is highly toxic and detrimental to the environment and human health, even at a low concentration of less than one ppm (Salleh et al., 2011; Mostafa Hosseini Asl et al., 2018; Ledakowicz and Gonera, 1999). It is necessary to reduce RhB to an acceptable concentration before it is introduced into the environment.

Many techniques have been adopted to effectively remove RhB from contaminated wastewater, including coagulation, ion exchange, flocculation, photocatalysis, adsorption, enzymatic reactions, and membrane separation (Bulut et al., 2008; Plácido et al., 2016; Mukhlish et al., 2016; La et al., 2020; Truong et al., 2020; Jadhav et al., 2020; Hao et al., 2020; Yao et al., 2020; Choudhury and Gogoi, 2021; Adekunle et al., 2020). At an industrial scale, all approaches have limitations. For example, treatment can be costly (adsorption method), expensive (depending on the pH solution), challenging to form radicals (chemical redox), form sludge, unsuitable for treating azo and reactive dyes effluents (coagulation), expensive and difficult to control efficiency (photocatalysis), time-consuming, of low performance and high pressure (ion exchange method), and expensive and incompatible (membrane separation) (Cates, 2017; Karcher et al., 2002; Dhiman et al., 2017). There is an urgent need to find inexpensive, sustainable, and effective treatment techniques for eliminating RhB from industrial wastewater.

Among other treatment technologies, adsorption is considered to be an affordable, reliable, and sustainable approach for removing organic dyes from wastewater because of its industrial-scale application, high efficiency, low cost, ability to treat dye-concentrated wastewater, and high efficiency (Hao et al., 2020; Yao et al., 2020; Liu et al., 2021; Jankowska et al., 2021; Ahmed et al., 2019). Many materials have been effectively employed as adsorbents to eliminate organic dyes, such as activated carbons, carbon nanotubes, biomass resources, polymers, graphene-based adsorbents, zeolites, and clay (Huang et al., 2019; Mezohegyi et al., 2012; Mashkoor and Nasar, 2020; Liu et al., 2019; Zhou et al., 2019; Kausar et al., 2018; Pala and Tokat, 2002; Mukurala et al., 2021). Among these, activated carbons have been extensively utilized for this method because of their high surface area, resistance to toxic chemicals, and low cost. One of the promising initial resources used to produce activated carbon is biomass, agricultural, and industrial waste (Udaiyappan et al., 2017; Lakshmi et al., 2018). Many studies have reported using sawdust (a biomass waste) as a starting material to produce activated carbon by a carbonization process, followed by chemical, physical, or combined processes (Akhouairi et al., 2019; Suganya et al., 2017). However, these sawdust-derived activated carbons have a low surface area, leading to low adsorption capability and a time-consuming adsorption process, which significantly hinders their practical application. Therefore, it is necessary to improve the surface area and adsorption time of activated carbon produced from sawdust.

Here, activated carbon with an ultra-high surface area was prepared from sawdust as a raw precursor material using a simple one-step chemical activation. The activating conditions were investigated to obtain sawdust activated carbon (sAC) with a high surface area and appropriate nanostructures for the rapid removal of organic dyes. The adsorption behavior of the resultant sAC toward RhB was investigated. The effects of pH solution, adsorption time, and adsorbent dosage on the removal efficiency were investigated and discussed.

2. Experimental section

2.1. Materials

The sawdust was obtained from a sawmill in Thai Binh province in Vietnam. The average size of the sawdust was approximately 1.4 mm. H_3PO_4 (85%), iodine, Rhodamine B (RhB), methylene blue (MB), and $Na_2S_2O_3$ were purchased from Xilong Chemicals (*Xilong* Scientific Co., Ltd, China). All chemicals, apart from the raw sawdust, were used as received without further purification.

2.2. Preparation of the activated carbon from the sawdust

The raw sawdust was ground to obtain a uniform particle size of 40–60 mesh and was then thoroughly washed and dried before conducting the experiment steps to fabricate activated carbon. The cleaned and dried sawdust was immersed in the 85% H_3PO_4 solution with a sawdust/H_3PO_4 weight ratio of 1/3 and was stirred gently at 95 °C for three hours. The H_3PO_4- impregnated sawdust was dried at 100 °C for 6 h. The sample was then transferred to a ceramic boat to perform the activation process at temperatures ranging from 400 to 1000 °C for various operating times of 30–60 min in CO_2 media. The resultant sawdust activated carbon was thoroughly washed with diluted NaOH and distilled water until the pH reached 7 and was then thoroughly dried at 105 °C for 2 h. The dried sawdust activated carbon was ground and stored for characterization and adsorption studies.

2.3. Characterizations of the prepared sawdust activated carbon

The morphologies of the prepared sAC were observed using a scanning electron microscope (M-EDX Hitachi S-4600, Japan) and transmission electron microscopy (TEM; JEOL JEM 1010). The functional groups on the surface of the sAC were investigated using Fourier transform infrared spectroscopy (FTIR, TENSOR II, Bruker Co., Germany). X-ray diffraction (XRD, X'Pert PRO PANalytical PW3040/60, Malvern Panalytical Co., the Netherlands) with a 0.15405 nm Cu-Kα radiation source was employed to study the crystallinity of the sample. The nitrogen adsorption–desorption approach using TriStar II Plus was used to determine the BET surface area. Samples were degassed at 110 °C for 4 h, and then nitrogen adsorption–desorption was conducted at −196 °C. Prior to measurement, the samples were degassed for 4 h at 250 °C to remove any adsorbed components. The iodine number of the sAC was determined using ASTM D-4607 as follows: first, iodine was adsorbed on the surface of the sAC until it reached equilibrium, and the iodine number was calculated. The adsorption performance of the sAC toward RhB or MB was investigated using a UV–Vis spectrophotometer to measure the peak intensity decrease at a wavelength of 553 nm for RhB and 668 nm for MB.

2.4. Adsorption study

Batch experiments at room temperature conducted the RhB and MB adsorption by the sAC. To determine the effect of the adsorption time, 10 mg of the sAC was added to 10 mL of the 10 ppm RhB or MB solutions, and nine samples were prepared under these conditions. Adsorption experiments were conducted at pH 7. After different time points from 30 s to 12 min. for RhB and 30 s to 5 min. for MB, each sample was removed, and the sAC was separated. The remaining RhB or MB concentration was then measured to determine the adsorption efficiency.

To determine the effect of the pH solution, 10 mg of the sawdust activated carbon was added to 10 mL of 10 ppm RhB at various pH solutions ranging from 1 to 11. Adsorption experiments were performed for 20 min to reach the equilibrium state. After adsorption, the sAC was collected from the supernatant by centrifugation, and RhB remaining in the solution was measured to determine the adsorption efficiency.

The RhB concentration on the adsorption efficiency of the sAC was also investigated as follows: 10 mg sAC was added to 10 mL RhB and MB at concentrations ranging from 10 to 80 ppm for RhB and 10 to 273 ppm for MB. Adsorption experiments were conducted at pH 7. After adsorption, the sAC was collected from the supernatant by centrifugation, and RhB remaining in the solution was measured to determine the adsorption efficiency.

The stability and reusability of the sAC for the RhB adsorption were investigated by the introduction of 10 mg sAC into 10 ml of RhB 10 ppm solution and shaken for 20 min to reach the equilibrium state. After adsorption, the sAC was collected from the supernatant by centrifugation, and RhB remaining in the solution was measured to determine the adsorption efficiency. The RhB dye was removed from the spent sAC by immersing in 20 ml ethanol and stirring for 10 min. The mixed solution was then centrifuged to separate activated carbon and RhB. The desorbed sAC was completely dried and repeated the adsorption experiment for the other 5 cycles. All the adsorption experiments were repeated three times to calculate the average value with standard derivations.

3. Results and discussion

It has been demonstrated that the concentration of the activating agents, temperature, and activating time are decisive factors in obtaining high-quality sawdust-activated carbons. Of these factors, the H_3PO_4 concentration has been extensively studied from previous works. Thus, in this study, the H_3PO_4: sawdust weight ratio of 1:3 was selected to fabricate the activated carbon. The effects of the activating temperature and time on the activated carbon surface area were investigated by determining the iodine number of the prepared sAC. Fig. 1 illustrates the effect of activating temperature and time on the surface area of the sAC. The activating temperature significantly affected the surface area of the as-prepared Sac (Fig. 1a). When the activating temperature increased, the iodine numbers increased, particularly with an activating temperature of higher than 600 °C, reaching a maximum of approximately 600 mg/g at 900 °C.

A further increase in the activating temperature resulted in a significant decrease in the quantity of sAC. Therefore, an activating temperature of 900 °C was selected as the optimal temperature for the fabrication of sAC. The activation time also affected the surface area of the sAC (Fig. 1b). Although the activation time on the surface area of the as-prepared activated carbon was negligible, an activation time of 60 min was chosen as the optimal time for the complete reaction between H_3PO_4 and the sawdust. Therefore, the sAC fabricated with an H_3PO_4: sawdust ratio of 1:3 activated at 900 °C for 60 min was used to characterize and investigate the adsorption behavior toward RhB.

The morphology of the as-prepared sAC obtained by activating the conditions of H_3PO_4: sawdust ratio of 1:3 at a temperature of 900 °C for 60 min was observed by scanning electron microscopy (SEM) (Fig. 2). At the low resolution of the SEM image (Fig. 2a), the sAC has a particle shape, with an average size of 1–5 μm. In the high-resolution SEM image (Fig. 2a), the surface of the sAC has a porous structure, comprising fine aggregated nanoparticles with diameters in the range of 10–20 nm (Fig. 2a). The highly porous structure of the obtained sAC was also confirmed by the TEM images (Fig. 2c). The fine particles on the surface of the sAC have sizes in the range of 10–20 nm (Fig. 2d).

Figure S1 shows the XRD patterns of the as-prepared sawdust activated carbon. The XRD pattern presents diffraction peaks at around 26° and 45°, which attributes to the (002) and (100) planes, respectively, of the graphitic crystalline

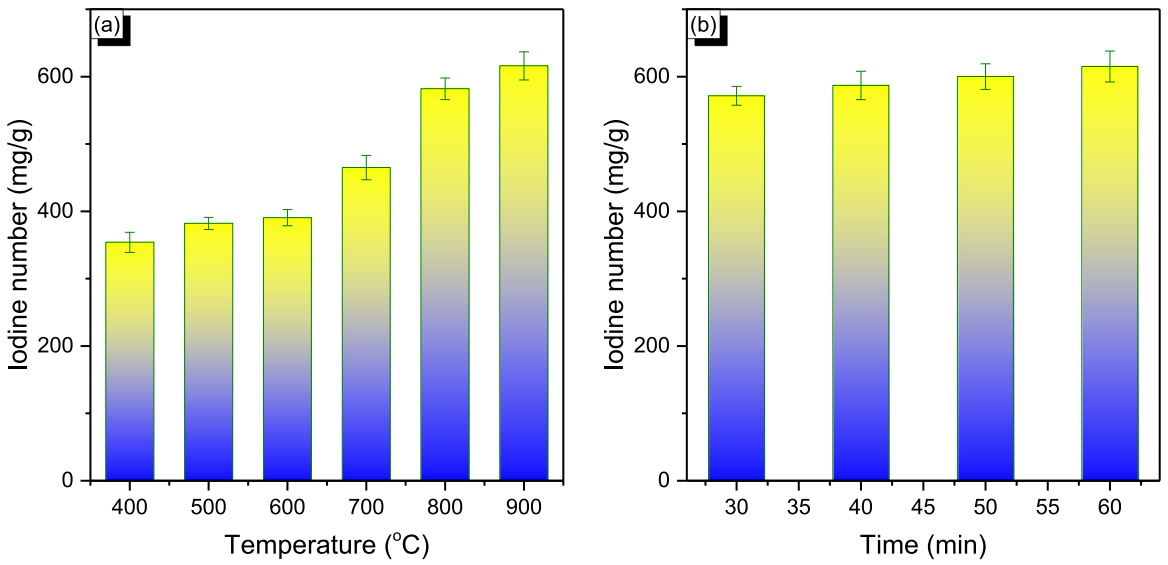

Fig. 1. Effect of the activating temperature (a) and time (b) on the surface area of the sawdust activated carbon.

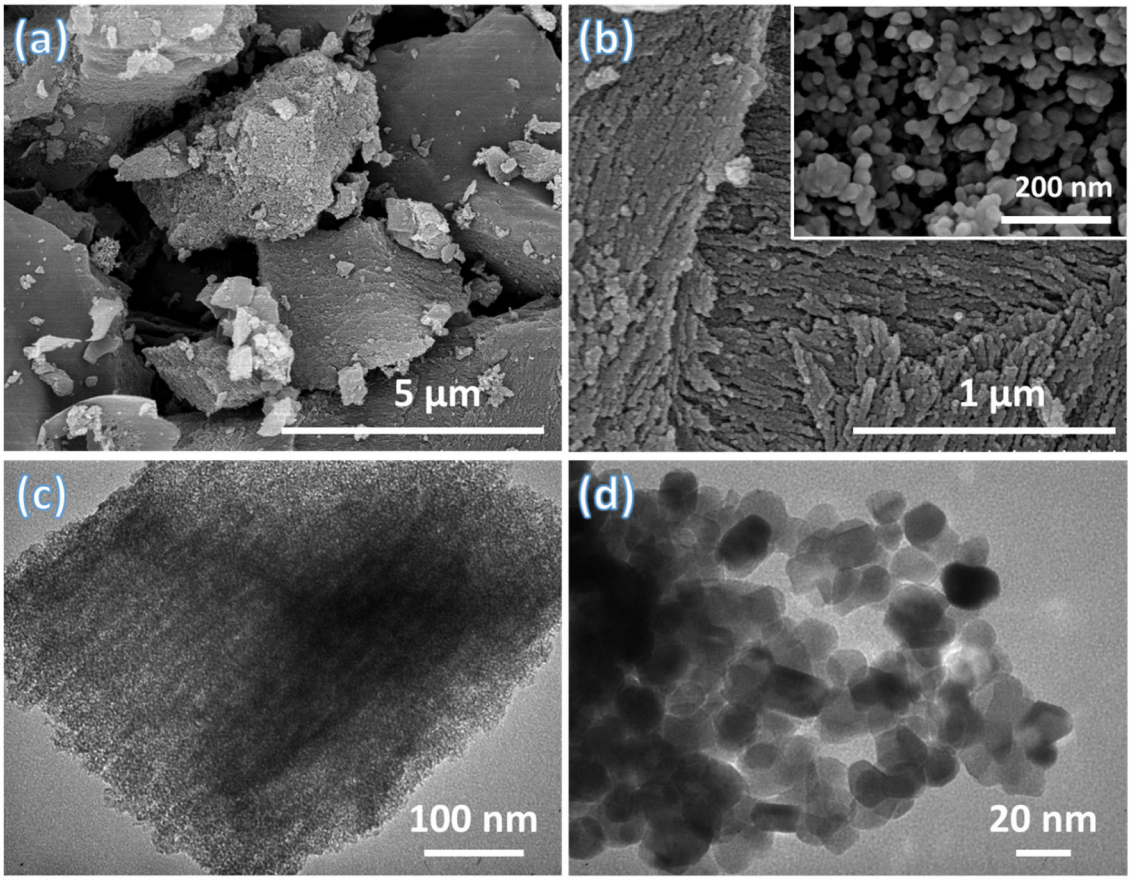

Fig. 2. Low (a) and High (b) resolution SEM images; Low (c) and High (d) resolution HR-TEM images of the sawdust activated carbon.

structure of the activated carbon (Shang et al., 2015). The activated carbon wall is graphitic, and therefore, more defects in the wall lead to a decrease in the graphite crystallinity of the activated carbon. As a result, the XRD diffraction peaks

Table 1
A comparison of the surface area of activated carbon prepared from sawdust.

Activating conditions	BET surface area, m^2/g	References
H_3PO_4, 400 °C, 30 min	293.13	Shah et al. (2020)
– Carbonization: 500 °C, 1 h – Activation: steam, 800 °C, 1 h	516.3	Malik (2004)
H_3PO_4, 600 °C, 3 h	1400	Kumar and Gupta (2020)
$CaCO_3$, 800 °C, 2 h	706.9	Kong et al. (2017)
$ZnCl_2$, $CaCO_3$, microwave, 10 min	941.08	Thue et al. (2017)
KOH, microwave, 10 min	952.23	Khasri and Ahmad (2018)
$ZnCl_2$, 550 °C, 30 min	999.65	Ramirez et al. (2020)
– Impregnation: H_3PO_4, 90 °C, 3 h – Activation: 900 °C, 1 h	1695	This work

are weaker. During the activation process, it is preferable to create more defects on the carbon wall because this would result in a high surface area of the activated carbon. In this case, the diffraction peaks of the sAC are relatively weak, which indicates that the sAC might have a high surface area. This claim is verified by measuring the BET surface area.

The chemical nature of the surface of the prepared sawdust activated carbon was investigated by FTIR spectroscopy (Figure S2). The sAC's FTIR spectrum reveals a characteristic peak at approximately 1141 cm^{-1}, which assigns to the appearance of phosphorous groups and/or aromatic phosphates in the activated carbon structure (Budinova et al., 2006; Shah et al., 2020). The vibration bands at 1564 cm^{-1} and 2365 cm^{-1} are attributed to the C-H and C=C sketching in the activated carbon (Ghouma et al., 2018; Izgi et al., 2019). The strong absorption peak at 3390 cm^{-1} can be assigned to the sketching vibration of O-H bending in the carboxylic groups after H_3PO_4 treatment and absorbed water in the activated carbon structure (Izgi et al., 2019; Nicholas et al., 2018). These results indicate that the prepared sawdust activated carbon consists of functional groups, suitable for the adsorption of organic compounds, including toxic dyes.

One of the most important properties of activated carbon, which is a decisive factor for the adsorption capability of carbon, is the surface area. Figure S3 shows the BET surface area plot of the sawdust activated carbon obtained with an H_3PO_4: sawdust ratio of 3:1 and activated at 900 °C for 60 min. The results show that the prepared sAC has an ultrahigh BET surface area of 1695 m^2/g, superior to that of the reported activated carbon prepared from sawdust. Table 1 shows the surface areas of the activated carbons prepared from sawdust under various activating conditions. The activated carbon prepared from sawdust activated by H_3PO_4 at 900 °C for 1 h in this study is higher than most sawdust-activated carbons reported in the literature.

Adsorption performance of the prepared sAC toward Rhodamine B

The adsorption time is an essential criterion for assessing the performance of an absorber. Fig. 3 shows the effect of the adsorption time on the removal efficiency of RhB by sawdust-activated carbon. The sAC displays rapid adsorption behavior toward RhB because the adsorption peaks of RhB disappear after 12 min of the batch adsorption experiment. After 2 min, more than 60% of RhB was absorbed by the activated carbon, and nearly 100% of RhB was completely removed from the aqueous solution after 10 min. This result indicates that the prepared sawdust activated carbon in this study exhibits relatively rapid adsorption behavior to remove RhB.

The effect of pH solutions on the adsorption behavior of an absorber is an important indicator for evaluating the applicability of activated carbon for practical wastewater treatment. In this study, the adsorption performance of the sAC toward RhB at various pH solutions, ranging from 1 to 11, was investigated for RhB removal by the sAC with an absorber dosage of 1 g/L and RhB concentration of 10 ppm (Fig. 4a). The sAC absorbed more than 90% of the RhB in all pH solutions. This result indicates that the sawdust-activated carbon in this study can be used as an effective absorber for the practical removal of RhB, without any additional costs for adjusting the pH solution.

Fig. 4b shows the effect of the RhB concentrations on the removal efficiency of the sAC with an absorber dosage of 1 g/L, and demonstrates that RhB removal efficiency decreases with increasing RhB concentration. While the sAC absorbed nearly 100% of RhB at a concentration of 10 ppm, the adsorption percentage decreased to 50% at an RhB concentration of 60 ppm, and in the experimental condition with an RhB concentration of 80 ppm, the RhB removal efficiency remained at approximately 40%. This result indicates that the prepared sAC can be effectively utilized to treat the RhB-contaminated solution with RhB concentrations of less than 30 ppm (removal efficiency higher than 80%). This range of RhB concentration remains significantly higher than the RhB concentration in real wastewater, and therefore the sAC prepared in this study could be employed for practical applications. With a higher RhB concentration, more absorbers or dilutions should be used.

Using the results of the effect of RhB concentrations on the removal efficiency by the sAC, the adsorption isotherm was studied following the Langmuir (1) and Freundlich models (2):

$$\frac{C_e}{Q_e} = \frac{C_e}{Q_{max}} + \frac{1}{Q_{max}K_L}. \tag{1}$$

$$\ln Q_e = \ln K_F + \frac{1}{n}\ln C_e, \tag{2}$$

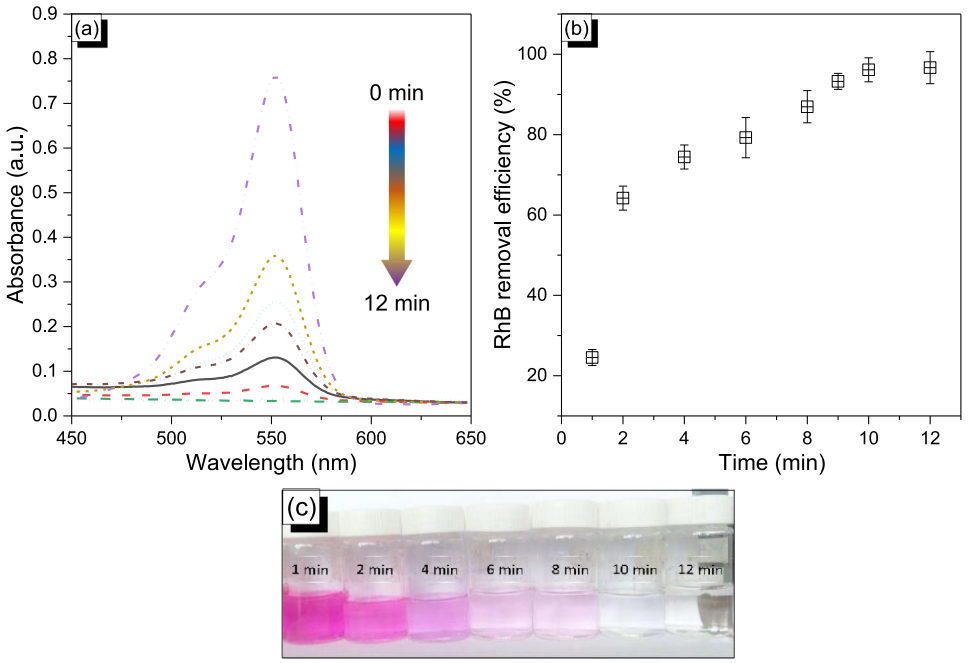

Fig. 3. Effect of the adsorption time on the RhB removal efficiency by the sAC with absorber dosage of 1 g/L and RhB concentration of 10 ppm.

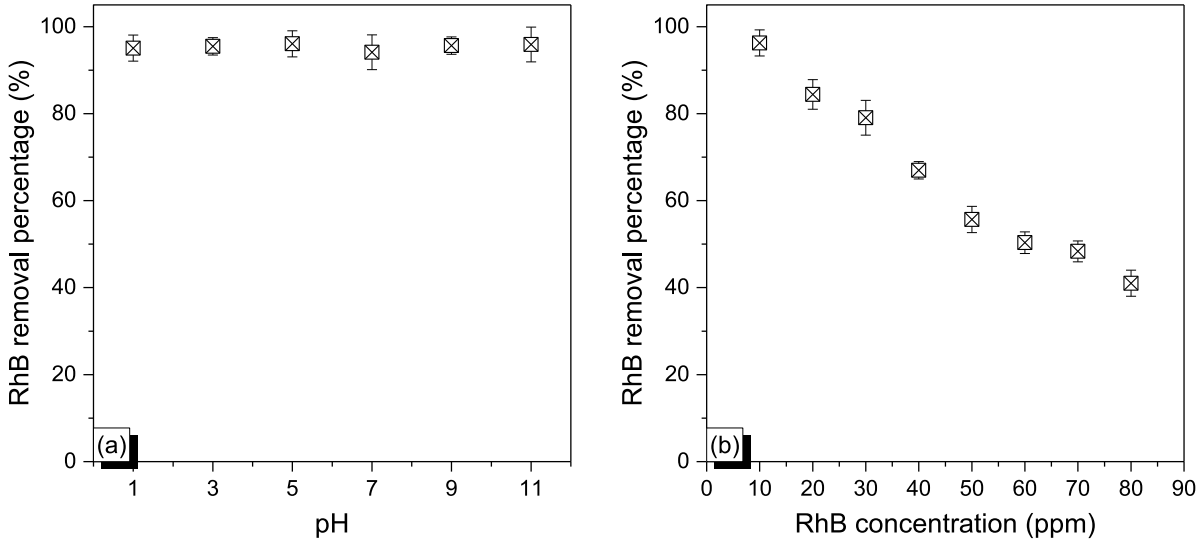

Fig. 4. Effect of pH solution (a) and RhB concentration s (b) on the removal efficiency of RhB by sAC under different conditions.

where C_e is the RhB concentration at equilibrium, Q_e is the absorbed RhB concentration by sAC, and n is the heterogeneity factor. Q_{max} is the maximal RhB adsorption capacity of the sAC, K_L is the Langmuir constant, and K_F is the Freundlich constant (Table 1) (Fig. 5).

The correlation coefficient obtained from the Langmuir model (0.98449) is higher than that of the Freundlich model (0.959) (Table 2), demonstrating that the Langmuir model is suitable for describing the adsorption behavior of the sAC toward RhB. This model indicates that RhB consistently absorbs on the surface of sAC at all sites, which is consistent with the chemisorption mechanism (Ding et al., 2014). In addition, the RL value is 0.445, demonstrating that the sAC favorably absorbed RhB. From the Langmuir model, the maximum adsorption capacity of the sAC for RhB was determined to be 35.7 mg/g sAC, which is reasonable for the practical utilization of sAC for the treatment of RhB-contaminated wastewater.

A comparative study on the removal efficiency of the sAC toward methylene blue (MB) dyes was also carried out. Illustrated in Figure S4 is the effect of the adsorption time on the removal performance of the sAC toward MB. sAC

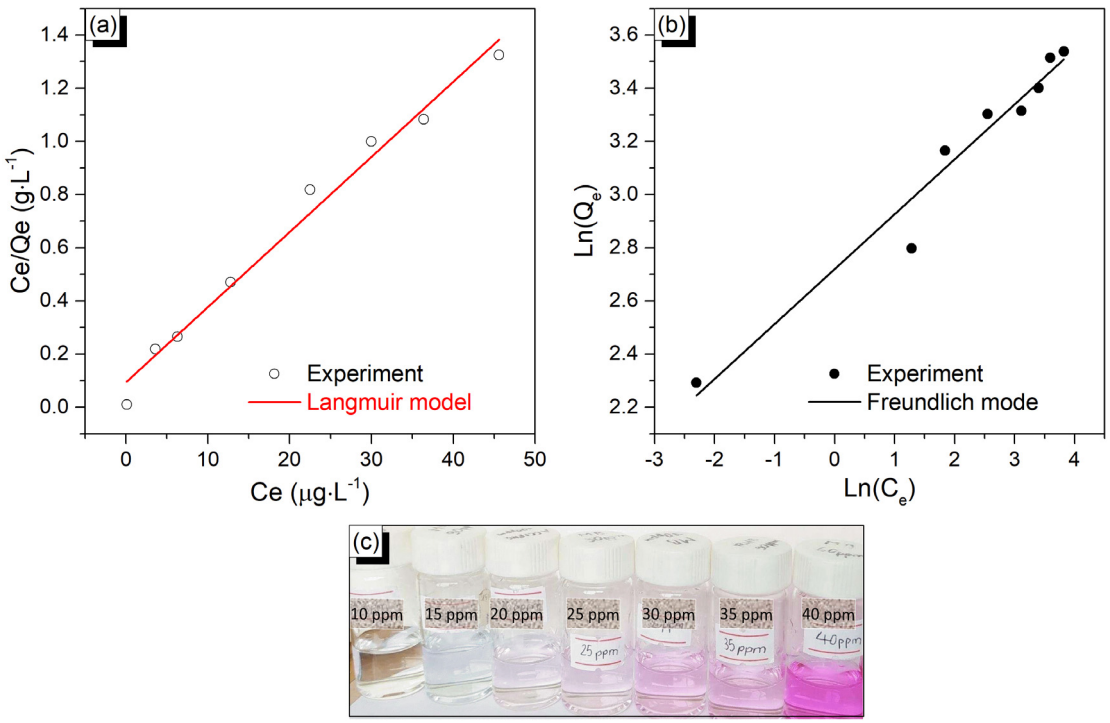

Fig. 5. (a) Langmuir and (b) Freundlich isotherm of the sawdust activated carbon toward RhB dye.

Table 2
Langmuir and Freundlich isotherm parameters for RhB adsorption by the sawdust activated carbon.

	Langmuir Model			Freundlich Model		
	Q_m (mg/g)	K_L (L/mg)	R^2	K_F	n	R^2
RhB	35.7	0.445	0.98449	15.165	5	0.959

exhibits an ultra-high adsorption rate for the MB that the sAC removed more than 96% of the MB after only 3 min of adsorption time, which is significantly higher than the adsorption performance of sAC toward RhB. Additionally, the sAC also revealed a superior adsorption capacity toward MB in comparison to RhB (Figure S5 & S6). The maximum adsorption capacity of sAC for the MB is calculated to be approximately 300 mg/g.

It demonstrated from the FTIR mentioned above that the sAC's surface contains OH and COOH functional groups, which control the adsorption behavior of the adsorbent. Because MB and RhB are cationic dyes, thus the adsorption mechanism could be presented as static interaction between the negative charge on the sAC's surface with the positive charge of the cationic dyes (Al-Degs et al., 2008). Thus, the dye molecules with strong alkalinity favor the adsorption capacity on the sAC's surface. The presence of the acidic group in the RhB molecules significantly hinders the static interaction between RhB and sAC; as a result, the RhB adsorption efficiency by the sAC is lower than that of MB dye (Jin et al., 2012).

The reusability of the adsorbents is one of the crucial factors for evaluating the applicability of the adsorbents in practice. Illustrated in Figure S7 is the recyclability of the sAC adsorbent for the RhB removal. It can be clearly seen that the RhB removal percentage by sAC negligibly decreases after five cycles of adsorption with around 10% of reduction, which demonstrates that the sAC could be employed as an effective adsorbent for the RhB removal in practical application.

4. Conclusion

Sawdust activated carbon, with an ultra-high surface area, was successfully fabricated by a simple one-step chemical activation process. The BET surface area of the prepared sawdust activated carbon obtained with an H_3PO_4/sawdust weight ratio of 3/1 activated at 900 °C for 60 min is 1695 m^2/g, which was superior to most of the activated carbon prepared from sawdust reported previously. The prepared sAC has a porous structure with graphitic crystallinity, consisting of aggregated nanoparticles with diameters ranging from 10 to 20 nm. The sAC displayed high and rapid adsorption behavior toward RhBs, with nearly 100% of RhB 10 ppm removed after 10 min. With this highly high effectiveness for removing organic dyes, the sawdust-activated carbon prepared in this study could be effectively utilized as an absorber for the practical treatment of dye-containing wastewater. Furthermore, the ultrahigh surface area of prepared sAC could be employed for the energy storage as a supercapacitor, which will be one of our research directions in future work.

CRediT authorship contribution statement

Van Hoang Nguyen: Investigation, Writing – original draft, Methodology, Formal analysis. **Dung T. Nguyen:** Investigation, Writing – original draft, Methodology, Data curation. **T. Tung Nguyen:** Investigation, Writing – original draft, Methodology. **H. Phuong T. Nguyen:** Supervision, Investigation, Conceptualization, Review & editing. **H. Binh Khuat:** Methodology, Resources, Review. **T. Hung Nguyen:** Methodology, Resources, Review & editing. **V. Khanh Tran:** Formal analysis, Review & editing. **S. Woong Chang:** Methodology, Resources, Review & editing. **Phuong Nguyen-Tri:** Methodology, Review. **D. Duc Nguyen:** Supervision, Conceptualization, Review & editing. **Duc Duong La:** Supervision, Investigation, Conceptualization, Review & editing.

Declaration of competing interest

The authors declare that they have no known competing financial interests or personal relationships that could have appeared to influence the work reported in this paper.

Acknowledgments

This research was supported in part by Hanoi University of Science and Technology-focused program, Vietnam (Project No. T2020-PC-214). The research collaboration among the groups, institutions, and universities of the authors is grateful.

Appendix A. Supplementary data

Supplementary material related to this article can be found online at https://doi.org/10.1016/j.eti.2021.101811.

References

Adekunle, A.S., Oyekunle, J.A.O., Durosinmi, L.M., Oluwafemi, O.S., Olayanju, D.S., Akinola, A.S., et al., 2020. Potential of cobalt and cobalt oxide nanoparticles as nanocatalyst towards dyes degradation in wastewater. Nano. Struct. Nano. Object. 21, 100405.
Ahmed, M.B., Johir, M.A.H., Zhou, J.L., Ngo, H.H., Nghiem, L.D., Richardson, C., et al., 2019. Activated carbon preparation from biomass feedstock: Clean production and carbon dioxide adsorption. J. Clean. Product. 225, 405–413.
Akhouairi, S., Ouachtak, H., Addi, A.A., Jada, A., Douch, J., 2019. Natural sawdust as adsorbent for the eriochrome black T dye removal from aqueous solution. Water Air Soil. Pollut. 230 (8), 1–15.
Al-Degs, Y.S., El-Barghouthi, M.I., El-Sheikh, A.H., Walker, G.M., 2008. Effect of solution pH, ionic strength, and temperature on adsorption behavior of reactive dyes on activated carbon. Dyes Pigment 77 (1), 16–23.
Budinova, T., Ekinci, E., Yardim, F., Grimm, A., Björnbom, E., Minkova, V., et al., 2006. Characterization and application of activated carbon produced by H3PO4 and water vapor activation. Fuel Process Technol 87 (10), 899–905.
Bulut, E., Özacar, M., Şengil, I.A., 2008. Equilibrium and kinetic data and process design for adsorption of Congo Red onto bentonite. J. Hazard. Mater. 154 (1–3), 613–622.
Cates, E.L., 2017. PHotocatalytic Water Treatment: So Where are We Going with This?. ACS Publications.
Choudhury, B.K., Gogoi, S.K., 2021. Reduced graphene oxide and Ag/AgCl composite (RGO–Ag/AgCl) for photocatalytic degradation of RhB using WLED. Nano. Struct. Nano. Object. 26, 100704.
Dhiman, N., Singh, A., Verma, N.K., Ajaria, N., Patnaik, S., 2017. Statistical optimization and artificial neural network modeling for acridine orange dye degradation using in-situ synthesized polymer capped ZnO nanoparticles. J. Colloid Interf. Sci. 493, 295–306.
Ding, L., Zou, B., Gao, W., Liu, Q., Wang, Z., Guo, Y., et al., 2014. Adsorption of Rhodamine-B from aqueous solution using treated rice husk-based activated carbon. Coll. Surf. A Physicochem. Eng. Asp 446, 1–7.
Ghouma, I., Jeguirim, M., Limousy, L., Bader, N., Ouederni, A., Bennici, S., 2018. Factors influencing NO2 adsorption/reduction on microporous activated carbon: porosity vs. surface chemistry. Materials 11 (4), 622.
Hao, M., Qiu, M., Yang, H., Hu, B., Wang, X., 2020. Recent advances on preparation and environmental applications of MOF-derived carbons in catalysis. Sci. Total Environ. 143333.
Huang, S., Wu, L., Li, T., Xu, D., Lin, X., Wu, C., 2019. Facile preparation of biomass lignin-based hydroxyethyl cellulose super-absorbent hydrogel for dye pollutant removal. Int. J. Biol. Macromol. 137, 939–947.
Izgi, M.S., Saka, C., Baytar, O., Saraçoğlu, G., ¸Sahin, Ö., 2019. Preparation and characterization of activated carbon from microwave and conventional heated almond shells using phosphoric acid activation. Anal. Lett 52 (5), 772–789.
Jadhav, R.W., La, D.D., More, V.G., Vo, H.T., Nguyen, D.A., Bhosale, S.V., 2020. Self-assembled kanamycin antibiotic-inorganic microflowers and their application as a photocatalyst for the removal of organic dyes. Sci. Rep. 10 (1), 1–8.
Jain, S., Shah, A.P., Shimpi, N.G., 2020. An efficient photocatalytic degradation of organic dyes under visible light using zinc stannate (Zn2SnO4) nanorods prepared by microwave irradiation. Nano. Struct. Nano. Object. 21, 100410.
Jankowska, K., Grzywaczyk, A., Piasecki, A., Kijeńska-Gawrońska, E., Nguyen, L.N., Zdarta, J., et al., 2021. Electrospun biosystems made of nylon 6 and laccase and its application in dyes removal. Environ. Technol. Innov 21, 101332.
Jayamani, G., Shanthi, M., 2020. An efficient nanocomposite CdS-ZnWO4 for the degradation of naphthol green B dye under UV-A light illumination. Nano. Struct. Nano. Object. 22, 100452.
Jin, Q.-Q., Zhu, X.-H., Xing, X.-Y., Ren, T.-Z., 2012. Adsorptive removal of cationic dyes from aqueous solutions using graphite oxide. Adsorpt. Sci. Technol. 30 (5), 437–447.
Kamranifar, M., Khodadadi, M., Samiei, V., Dehdashti, B., Sepehr, M.N., Rafati, L., et al., 2018. Comparison the removal of reactive red 195 dye using powder and ash of barberry stem as a low cost adsorbent from aqueous solutions: Isotherm and kinetic study. J. Mol. Liq 255, 572–577.
Karcher, S., Kornmüller, A., Jekel, M., 2002. Anion exchange resins for removal of reactive dyes from textile wastewaters. Water Res. 36 (19), 4717–4724.
Kausar, A., Iqbal, M., Javed, A., Aftab, K., Bhatti, H.N., Nouren, S., 2018. Dyes adsorption using clay and modified clay: a review. J. Mol. Liq. 256, 395–407.

Khasri, A., Ahmad, M.A., 2018. Adsorption of basic and reactive dyes from aqueous solution onto intsia bijuga sawdust-based activated carbon: batch and column study. Environ. Sci. Pollut. Res 25 (31), 31508–31519.
Kong, L., Su, M., Peng, Y., Liu, J., Li, H., Diao, Z., et al., 2017. Producing sawdust derived activated carbon by co-calcinations with limestone for enhanced Acid Orange II adsorption. J. Clean. Prod. 168, 22–29.
Kumar, A., Gupta, H., 2020. Activated carbon from sawdust for naphthalene removal from contaminated water. Environ. Technol. Innov. 20, 101080.
La, D.D., Tran, C.V., Hoang, N.T., Ngoc, M.D.D., Nguyen, T.P., Vo, H.T., et al., 2020. Efficient photocatalysis of organic dyes under simulated sunlight irradiation by a novel magnetic CuFe2O4@ porphyrin nanofiber hybrid material fabricated via self-assembly. Fuel 281, 118655.
Lakshmi, S.D., Avti, P.K., Hegde, G., 2018. Activated carbon nanoparticles from biowaste as new generation antimicrobial agents: A review. Nano. Struct. Nano. Object. 16, 306–321.
Ledakowicz, S., Gonera, M., 1999. Optimisation of oxidants dose for combined chemical and biological treatment of textile wastewater. Water Res 33 (11), 2511–2516.
Liu, X., Pang, H., Liu, X., Li, Q., Zhang, N., Mao, L., et al., 2021. Orderly porous covalent organic frameworks-based materials: superior adsorbents for pollutants removal from aqueous solutions. Innovation 100076.
Liu, H., Sun, R., Feng, S., Wang, D., Liu, H., 2019. Rapid synthesis of a silsesquioxane-based disulfide-linked polymer for selective removal of cationic dyes from aqueous solutions. Chem. Eng. J. 359, 436–445.
Malik, P., 2004. Dye removal from wastewater using activated carbon developed from sawdust: adsorption equilibrium and kinetics. J. Hazard Mater. 113 (1–3), 81–88.
Manzoor, J., Sharma, M., 2020. Impact of Textile Dyes on Human Health and Environment. Impact of Textile Dyes on Public Health and the Environment. IGI Global, pp. 162–169.
Mashkoor, F., Nasar, A., 2020. Carbon nanotube-based adsorbents for the removal of dyes from waters: a review. Environ. Chem. Lett. 18 (3), 605–629.
Mezohegyi, G., van der Zee, F.P., Font, J., Fortuny, A., Fabregat, A., 2012. Towards advanced aqueous dye removal processes: a short review on the versatile role of activated carbon. J. Environ. Manag. 102, 148–164.
Mostafa Hosseini Asl, S., Ghadi, A., Sharifzadeh Baei, M., Javadian, H., Maghsudi, M., Kazemian, H., 2018. Porous catalysts fabricated from coal fly ash as cost-effective alternatives for industrial applications: A review. Fuel 217, 320–342.
Mukhlish, M., Khan, M., Islam, A., Akanda, A., 2016. Removal of reactive dye from aqueous solution using coagulation–flocculation coupled with adsorption on papaya leaf. J. Mech. Eng. Sci. 10 (1), 1884–1894.
Mukurala, N., Mokurala, K., Suman, S., Kushwaha, A.K., 2021. Synthesis of porous Cu2FeSnS4 particles via solvothermal process for removal of organic acid fuchsin dye pollutant from wastewater. Nano. Struct. Nano. Object. 26, 100697.
Nicholas, A.F., Hussein, M.Z., Zainal, Z., Khadiran, T., 2018. Palm kernel shell activated carbon as an inorganic framework for shape-stabilized phase change material. Nanomaterials 8 (9), 689.
Pala, A., Tokat, E., 2002. Color removal from cotton textile industry wastewater in an activated sludge system with various additives. Water Res 36 (11), 2920–2925.
Plácido, J., Chanagá, X., Ortiz-Monsalve, S., Yepes, M., Mora, A., 2016. Degradation and detoxification of synthetic dyes and textile industry effluents by newly isolated leptosphaerulina sp. from Colombia. Biores Bioprocess 3 (1), 1–14.
Ramirez, A., Ocampo, R., Giraldo, S., Padilla, E., Flórez, E., Acelas, N., 2020. Removal of Cr (VI) from an aqueous solution using an activated carbon obtained from teakwood sawdust: kinetics, equilibrium, and density functional theory calculations. J. Environ. Chem. Eng. 8 (2), 103702.
Robinson, T., McMullan, G., Marchant, R., Nigam, P., 2001. Remediation of dyes in textile effluent: a critical review on current treatment technologies with a proposed alternative. Bioresour. Technol 77 (3), 247–255.
Salleh, M.A.M., Mahmoud, D.K., Karim, W.A.W.A., Idris, A., 2011. Cationic and anionic dye adsorption by agricultural solid wastes: A comprehensive review. Desalination 280 (1–3), 1–13.
Sarkar, N., Sahoo, G., Swain, S.K., 2020. Nanoclay sandwiched reduced graphene oxide filled macroporous polyacrylamide-agar hybrid hydrogel as an adsorbent for dye decontamination. Nano. Struct. Nano. Object. 23, 100507.
Shah, J.A., Butt, T.A., Mirza, C.R., Shaikh, A.J., Khan, M.S., Arshad, M., et al., 2020. Phosphoric acid activated carbon from melia azedarach waste sawdust for adsorptive removal of reactive orange 16: Equilibrium modelling and thermodynamic analysis. Molecules 25 (9), 2118.
Shang, H., Lu, Y., Zhao, F., Chao, C., Zhang, B., Zhang, H., 2015. Preparing high surface area porous carbon from biomass by carbonization in a molten salt medium. RSC Adv. 5 (92), 75728–75734.
Suganya, S., Saravanan, A., Ravikumar, C., 2017. Computation of adsorption parameters for the removal of dye from wastewater by microwave assisted sawdust: theoretical and experimental analysis. Environ. Toxicol. Pharmacol. 50, 45–57.
Thue, P.S., dos Reis, G.S., Lima, E.C., Sieliechi, J.M., Dotto, G.L., Wamba, A.G., et al., 2017. Activated carbon obtained from sapelli wood sawdust by microwave heating for o-cresol adsorption. Res. Chem. Intermed 43 (2), 1063–1087.
Truong, N.T., Thi, H.P.N., Ninh, H.D., Phung, X.T., Van Tran, C., Nguyen, T.T., et al., 2020. Facile fabrication of graphene@ Fe-Ti binary oxide nanocomposite from ilmenite ore: An effective photocatalyst for dye degradation under visible light irradiation. J. Water Process Eng. 37, 101474.
Udaiyappan, A.F.M., Hasan, H.A., Takriff, M.S., Abdullah, S.R.S., 2017. A review of the potentials, challenges and current status of microalgae biomass applications in industrial wastewater treatment. J. Water Process Eng. 20, 8–21.
Yao, L., Yang, H., Chen, Z., Qiu, M., Hu, B., Wang, X., 2020. Bismuth oxychloride-based materials for the removal of organic pollutants in wastewater. Chemosphere 128576.
Zhou, Y., Lu, J., Zhou, Y., Liu, Y., 2019. Recent advances for dyes removal using novel adsorbents: a review. Environ. Pollut. 252, 352–365.